Surface & Coatings Technology 204 (2010) 3280–3286

Contents lists available at ScienceDirect

Surface & Coatings Technology

journal homepage: www.elsevier.com/locate/surfcoat

Corrosion behavior of martensitic and precipitation hardening stainless steels treated by plasma nitriding

Sonia P. Brühl [a,*], Raúl Charadia [a], Silvia Simison [b], Diego G. Lamas [c], Amado Cabo [d]

[a] Surface Engineering Group, Universidad Tecnológica Nacional, FRCU, Ing. Pereira 676, E3264BTD Concepción del Uruguay, Argentina
[b] INTEMA, División Corrosión, Universidad Nacional de Mar del Plata, Juan B. Justo 4302, B7608FDQ Mar del Plata, Argentina
[c] Centro de Investigaciones en Sólidos (CINSO), CITEFA–CONICET, J.B. de La Salle 4397 (B1603ALO) Villa Martelli, Pcia. de Buenos Aires, Argentina
[d] IONAR S.A., Arias 3422, C1430CRB Ciudad de Buenos Aires, Argentina

ARTICLE INFO

Article history:
Received 25 November 2009
Accepted in revised form 18 March 2010
Available online 27 March 2010

Keywords:
Plasma nitriding
PH stainless steel
Martensitic stainless steel
Corrosion resistance

ABSTRACT

Plasma nitriding is a well established technology to improve wear and corrosion properties of austenitic stainless steels. Nevertheless, in the case of martensitic stainless steels, it continues being a problem mainly from the corrosion resistance viewpoint.
In this work, three high chromium stainless steels (M340, N695 and Corrax) were hardened by ion nitriding at low temperature, intending to preserve their corrosion resistance.
Corrosion behavior was evaluated by $CuSO_4$ spot, salt spray fog and potentiodynamic polarization in NaCl solution. Microstructure was analyzed by optical microscopy, SEM (EDS) and glancing angle X-ray diffraction. All the samples showed an acceptable corrosion resistance in experiments with $CuSO_4$, but in salt spray fog and electrochemical tests, only Corrax showed good behavior. The poor corrosion performance could be explained by chromium carbides formed in thermal treatment stage in martensitic steels and chromium nitrides formed during nitriding, even though the process was carried out at low temperature.

1. Introduction

Plasma surface engineering gathers a group of different techniques oriented to modify a material surface. One of these techniques is plasma nitriding, especially when using a DC pulsed power supply. This is a plasma assisted thermochemical process, in which the workpiece acts as a cathode. The ion bombardment heats the workpiece, cleans the surface and provides active nitrogen. As a result, the hardness achieved on the surface is the highest and its value decreases with depth until the core hardness is reached. This surface modification improves its load bearing capacity. Ion nitriding has proved to be a suitable hardening process for stainless steels, improving wear resistance [1–4]. Providing with a good control of process parameters such as temperature and process time, corrosion resistance of austenitic stainless steels can be unaltered and even improved due to the formation of the so called "S" phase, which is a nitrogen supersaturated expanded austenitic phase [5,6].

In the case of martensitic stainless steels, however, corrosion resistance is still an issue, because of their low chromium content and the formation of chromium carbides, during heat treatment and chromium nitrides during nitriding. These steels should be nitrided after quenching and tempering, because mechanical properties on the bulk are as important as surface hardening. There are several reports in the literature for AISI 410 and 420 [7–9], and for precipitation hardening (PH) stainless steels [10–12] that present some promising results if a low temperature process (around 350 °C–380 °C) is applied. The PH stainless steels could be better candidates for plasma nitriding, because they do not need to go through the quenching and tempering treatment; they only need an aging treatment around 500 °C, to obtain their hardness and mechanical properties, based on the formation of fine precipitates. Besides, they have low carbon content and chromium carbides precipitation could be reduced. On the other hand, high chromium (17 wt.%) martensitic stainless steel could improve its hardness by nitriding and preserve its corrosion resistance as well.

In this work, three high chromium stainless steels designed for corrosive applications which can be hardened by thermal treatment to achieve high hardness and wear resistance were selected to be nitrided and study their corrosion resistance after the process. As they are recommended for corrosive applications, the aim of this work was to study the effect of the nitriding treatment on their corrosion resistance, particularly in relation to their microstructure.

2. Material and methods

Disc samples 6 mm in height and 24 mm in diameter were sliced from a bar stock for the three steels. Planar faces were ground and

* Corresponding author. Universidad Tecnológica Nacional, Facultad Regional Concepción del Uruguay, E3264BTD Concepción del Uruguay, Argentina. Tel./fax: 0054 3442 425541/423803.
E-mail addresses: sonia@frcu.utn.edu.ar (S.P. Brühl), charadia@frcu.utn.edu.ar (R. Charadia), ssimison@fi.mdp.edu.ar (S. Simison), dlamas@citefa.gov.ar (D.G. Lamas), info@ionar.com.ar (A. Cabo).

0257-8972/$ – see front matter © 2010 Elsevier B.V. All rights reserved.
doi:10.1016/j.surfcoat.2010.03.036

polished with successively finer emery paper and diamond paste, down to 1 μm; only one face was nitrided.

M340 is a martensitic stainless steel from Boehler is used in plastic nozzles and pistons, mold inserts, cutting tools and screws, where abrasive wear resistance is necessary. It has good hardenability and high hardness (550–600 HV) after quenching. N695 is also a martensitic stainless steel provided by the same firm and it is similar to AISI 440C, used in balls, rollers, needles and rings for corrosion resistant bearings.

Finally, Corrax is a precipitation hardening steel used in injection molds for corrosive plastics, rubber and parts for medical and food industry, also in extrusion dies and engineering parts for plastic processing. This steel has a wide hardness range, 340–520 HV, achieved by an aging treatment in the temperature range 425–600 °C, has extremely good dimensional stability during the aging process, high uniformity of properties even in large dimensions and a very good weldability. Normally its corrosion resistance is superior to AISI 420 and AISI 440C.

The three different steels have been plasma nitrided in a DC pulsed discharge facility after heat treatment. Hardness, microstructure and corrosion resistance were analyzed for the three steels and compared before and after plasma processing.

The nominal composition of the studied steels is presented in Table 1.

The martensitic steels were received in the annealed condition (ferritic matrix with $M_{23}C_6$ carbide dispersion); consequently, the samples were heat treated as recommended by supplier. The M340 and N695 samples were austenitised at 1030 °C for 20 min, oil quenched and tempered at 320 °C for 2 h. In these conditions a martensitic structure was obtained. Corrax samples were aged at 530 °C for 2 h; in this case, also a martensitic structure was obtained.

The nitriding facility was designed and constructed at the UTN and it has been described elsewhere [13] but it is, essentially, a steel chamber where the samples are placed in cavities over the cathode and a cylinder acts as the anode of a DC pulsed discharge. Current density, voltage bias and partial pressures of work gases can be adjusted, and temperature can be set and controlled separately by a heat resistance array around the cathode and a PID controller. Sputter cleaning was performed in Ar–H_2 atmosphere at about 100 °C for 2 h, in order to remove the oxide layers formed on the surface of the samples. Nitriding was carried out for 10 h in a 22% N_2–H_2 mixture at a temperature of 360 °C. The mean voltage between electrodes was set at 450 V, in a DC pulsed mode of 500 Hz frequency and a duty factor of 35%. The mean current density was 0.1 mA/cm^2.

Before and after plasma treatment, the sample's surface was tested with copper sulfate spot to analyze passivity according to ASTM standard A967-05, practice D. Surface was swabbed for 6 min with pent hydrated copper sulfate ($CuSO_4 \cdot 5H_2O$) and observed after the test to detect copper deposition, which would indicate the presence of free iron.

In order to study the layers microstructure, samples were cut, hot mounted, ground and polished, and finally etched with Vilella's reagent [14]. Optical microscopy and SEM were used to observe modified layers. The crystalline phases were identified by X-ray diffraction (XRD) using a Philips PW3710 diffractometer operated with Cu–Kα radiation. The analysis was performed in glancing angle geometry using a Philips thin film attachment. The angle of incidence was set at 1°, corresponding to an X-ray penetration depth of about 0.6 μm for all the studied steels.

Salt fog spray tests were conducted in a self made chamber according to ASTM B117 [15]. The solution used for salt spray was 5% NaCl of ph 6.8 and the experiments were carried out at a temperature of 32 °C, during 100 h. Results were evaluated qualitatively, observing the presence of rust, and quantitatively, after taking a digital photograph. The photographs were analyzed with the software Scion Image® to obtain the percentage of the surface covered with corrosion products after the test. Pits with areas larger than 0.1 mm^2 were also detected and counted.

Electrochemical experiments were conducted at room temperature and atmospheric pressure in a three-electrode cell. A saturated calomel electrode (SCE) was employed as the reference electrode and a platinum spiral wire as the counter electrode. So as to avoid altering ground surface, the samples were pressed against the bottom of the cell and sealed using an O-ring [16]. The resulting working electrode area was 0.41 cm^2. A 3.5 wt.% NaCl air saturated solution was used (air was continuously bubbled in the solution in order to get saturation concentration). The anodic curves were used to compare the behavior of the different samples respect to their resistance to localized corrosion (pitting and/or crevice) and were repeated at least 3 times. Corrosion potential was monitored for 40 min after which anodic polarization test was carried out at a 1 mV/s sweep rate up to an arbitrarily chosen current density of 50 μA/cm^2 in order to analyze the morphology of the attack at constant degree of dissolution and to compare results with those obtained in the salt spray fog test. The corresponding potential was called E_{50}.

Common practice for comparing the vulnerability of various alloys to localized corrosion in a given environment involves cyclic potentiodynamic polarization. The working electrode potential is scanned of from a low value, such as the corrosion potential, to more positive potential values. The reversal of the potential is done at a fixed, arbitrary chosen current density. During upward scanning, breakdown occurs where the current increases sharply from the passive current level and pits start growing. This potential is called breakdown or pitting potential (E_{bd}). On reversal of the scan direction, pits repassivate where the current drops back to low values representative of passive dissolution at the protection or repassivation potential (E_r). It is generally considered that materials exhibiting higher values of E_{bd} and E_r are more resistant to localized corrosion [17].

In this work, cyclic potentiodynamic polarization was carried out only in Corrax samples. The sweep direction was inverted when the current density reached 200 μA/cm^2. The corresponding potential was called E_{200}.

Table 1
Composition in weight percentage of the different steels used in this study (Fe balance).

Steel/wt.%	C	Cr	Mo	Mn	Si	Ni	Others
Corrax	0.03	12.0	1.4	0.3	0.3	9.2	Al
N695	1.05	17.0	0.5	0.4	0.4	–	
M340	0.54	17.3	1.1	0.4	–	–	N

3. Results

3.1. Surface aspect and $CuSO_4$ spot

After plasma nitriding, the surfaces of the samples were slightly polished with diamond paste to remove any oxide formed during the cooling phase. It was proved that no change in hardness is produced by this procedure. After that, the first study of corrosion was the $CuSO_4$ spot test. As already mentioned the presence of copper as a deposit on the surface indicates the presence of free iron, indicating incomplete passivation.

All heat treated samples, prior to nitriding, did not show sensitization, after 6 min of pent hydrated $CuSO_4$. In the case of nitrided samples, Corrax showed the same behavior but in M340 and N695 nitrided samples, copper deposition was observed in less than a minute.

3.2. Microstructure and hardness

In order to observe the microstructure samples were etched with Vilella's reagent for 60 s. Their microstructures were observed with an optical microscope. Fig. 1 shows three micrographs, where a white layer can be observed on the surface, and below is the martensitic structure of the bulk. In the case of Corrax PH steel, it is observed in Fig. 1a that the white layer penetrates along the grain boundaries but in the three steels the white layer showed no sharp interface as it normally observed in the case in nitrided austenitic stainless steel [2–4]. In the case of N595 and M340 steels, some white and rounded structures can also be observed; which correspond to carbides formed during the heat treatment. This white nitrided layer was not attacked by the used reagent, whereas the substrate or the bulk material was etched. No signs of dark sublayers could be observed above the white layer, meaning that precipitation of Fe_4N and CrN did not occur, at least massively, as it happens when martensitic stainless steels are nitrided at 450 °C or 500 °C [7,8,13,18].

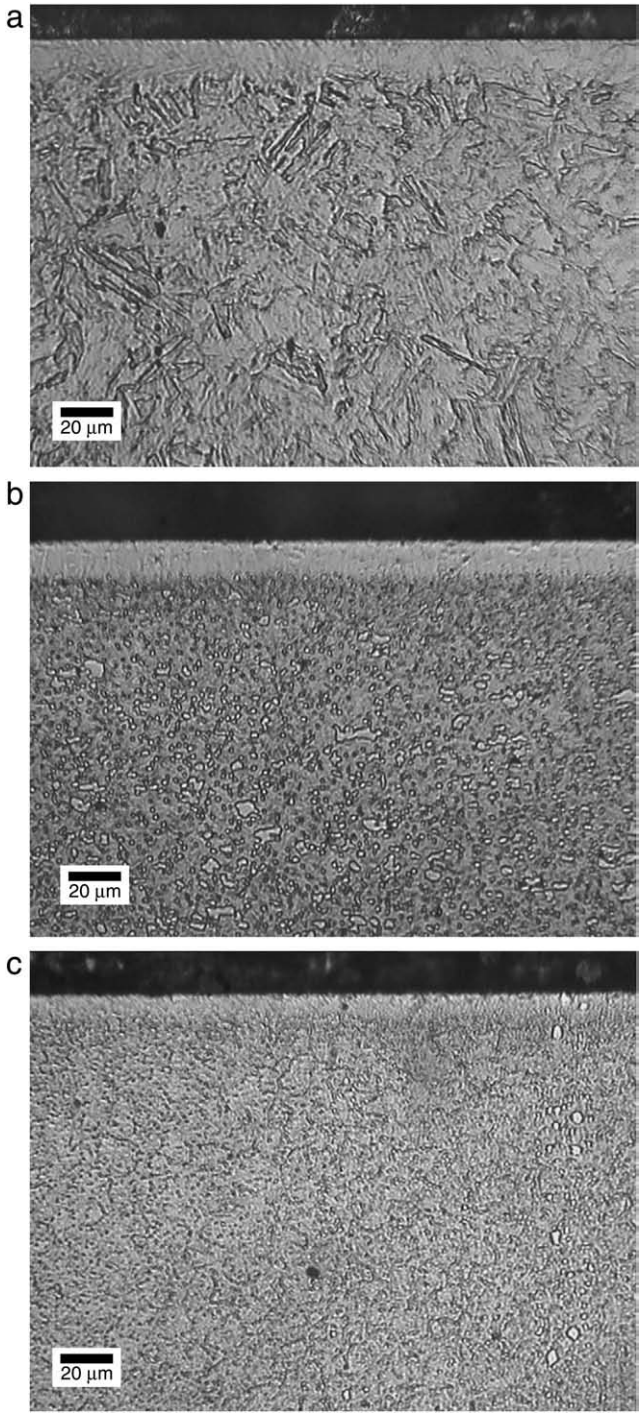

Fig. 1. Nitrided layers with 400× magnification. a) Corrax, b) N695, c) M340.

The hardness of all samples before and after nitriding and the white nitrided layer width are presented in Table 2. As hardness fell drastically below this layer, reaching the bulk hardness at 50 µm depth, only the white layer was considered the "nitrided layer".

Based on different published works it is recognized that the white layer in nitrided martensitic steels is a stressed structure called "expanded martensite" [19–21]. However, this nomenclature is not very suitable since martensite is a stressed structure itself, therefore "expanded ferrite" could be a more appropriate name [7].

Glancing angle XRD analysis revealed a martensite structure in the three studied steels, as it can be concluded from the positions of the Fe α peaks. But it is also observed an amount of retained austenite that was converted into expanded austenite γ_N after nitriding, so as other authors' observations [11]. XRD information comes from a shallow subsurface layer which is the zone of major concentration of nitrogen. It was found by Frandsen at al. [19] and also by Li et. al. [22], who worked with Corrax nitriding, that for nitrogen activities above a certain threshold value the transformation of b.c.t. (α'_N) to f.c.c. (γ_N) occurs, because of the stabilizing effect of nitrogen on austenite.

After nitriding the Corrax samples there was no sign of Fe nitrides or carbides (Fig. 2a) but it can be noticed that the Fe α peaks are shifted to lower angles, showing a lattice expansion. In N595 and M340 samples, on the other side, Cr carbides were observed even before nitriding. After nitriding, not only the Fe α lattice was expanded but also Cr nitrides and γ nitrides were detected (Figs. 2b and c).

A SEM micrograph of the etched surface shows that carbides are located mainly at grain boundaries of the previous austenite of the N695 steel (Fig. 3a). Composition analysis of these precipitates was carried out by EDS, showing a much higher concentration of chromium than iron (Fig. 3b). This is consistent with the observations of other authors [23].

3.3. Salt spray fog test

After the 100 h salt spray test, nitrided and non nitrided samples of the three steels were photographed to determine the presence of rust and evaluate the percentage of surface covered with corrosion. Pictures of all samples are presented in Fig. 4. It can be observed, that corrosion resistance of nitrided N695 and M340 diminished respect to the non nitrided materials, which was only heat treated. Red rust and severe localized corrosion could be observed in these steels. However, Corrax results indicate that corrosion resistance was preserved after nitriding.

The samples were then cleaned and polished to remove the corrosion products and to be able to observe the presence of pits. Using the optical microscope with low magnification (100×) and with the aid of the Scion Image® software, only pits with an area greater

Table 2
Surface hardness of all the samples – measured with Vickers indenter and 50 g load – and the width of the nitrided layer.

Steel sample	Hardness before nitriding	Hardness after nitriding	Nitrided layer width
Corrax	580 ± 50	1290 ± 110	10–12 µm
N695	640 ± 60	1130 ± 110	14–15 µm
M340	630 ± 60	1100 ± 100	9–10 µm

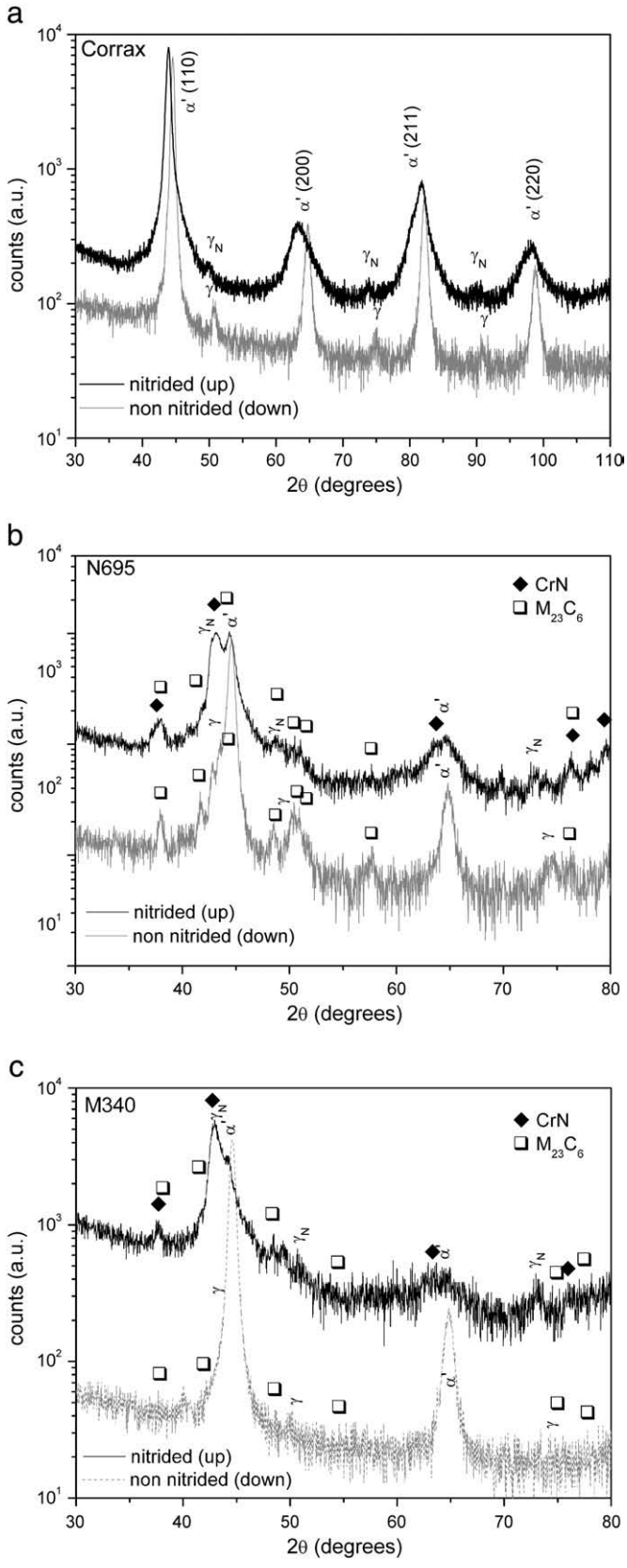

Fig. 2. Glancing angle X-ray diffractograms (in logarithmic scale) before and after nitriding. a) Corrax samples, b) N695 samples, c) M340 samples.

than 0.1 mm^2 were selected and counted. This size is the smallest in the corrosion chart of ASTM Standard G46. Quantitative results are presented in Table 3.

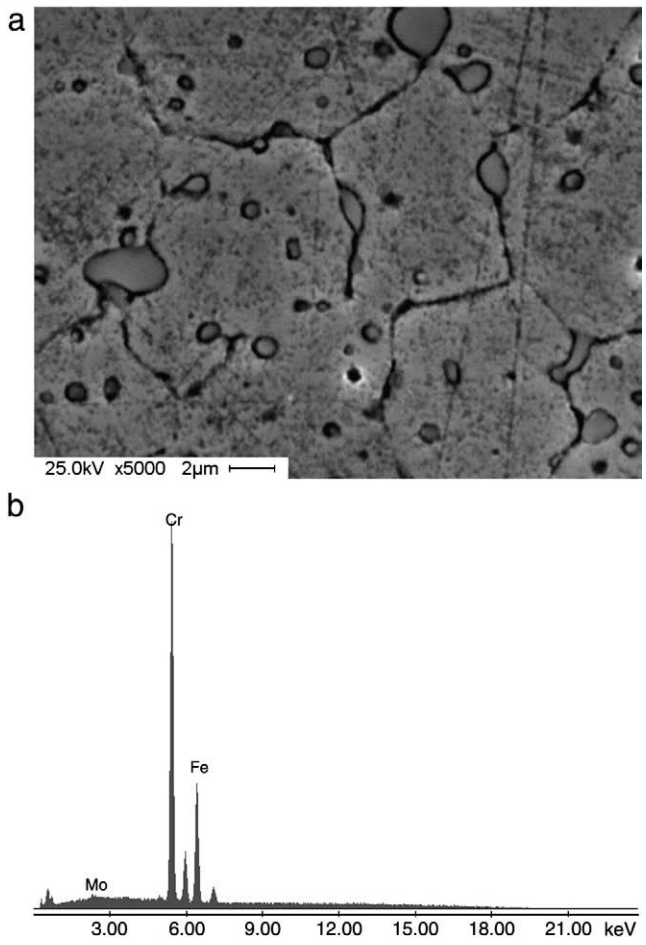

Fig. 3. a) SEM micrograph of the N695 nitrided surface etched with Vilella's reagent, where carbides precipitation is observed at grain boundaries of the previous austenite. b) EDS analysis of a carbide precipitate.

3.4. Electrochemical tests

In a first experiment the corrosion potential evolution E_{corr} was measured in an open circuit potential configuration. The sample was immersed long enough for the corrosion potential to reach steady state. Each sample was tested between three and four times in different regions of the surface and free corrosion potential–time curves were recorded for 40 min. A corrosion potential E_{corr} mean value of the steady state for each condition was calculated and presented in the last column of Table 3. It is observed that E_{corr} values for Corrax samples have no remarkable differences between nitrided or non nitrided samples which are in agreement with values found in the literature for this kind of steels [11]. In martensitic stainless steels, however, their corrosion potentials shift to less noble values, and nitrided samples have even more negative potentials than non nitrided samples.

The detrimental effect of nitriding can be observed in Fig. 5. The anodic slopes for the nitrided samples were lower and the current densities higher compared to the non nitrided same material. Potentials at the end of the scanning (E_{50}) were also lower for nitrided samples.

It is also shown in Fig. 5 that martensitic stainless steels have a different behavior from that of Corrax. For M340 and N695 samples, the anodic slopes were clearly lower and part of the attack was found under the O-ring, indicating that these samples were more susceptible to localized corrosion.

On the other hand, Corrax anodic curves show a “passive-like” range, with nearly similar values of current densities for both nitrided

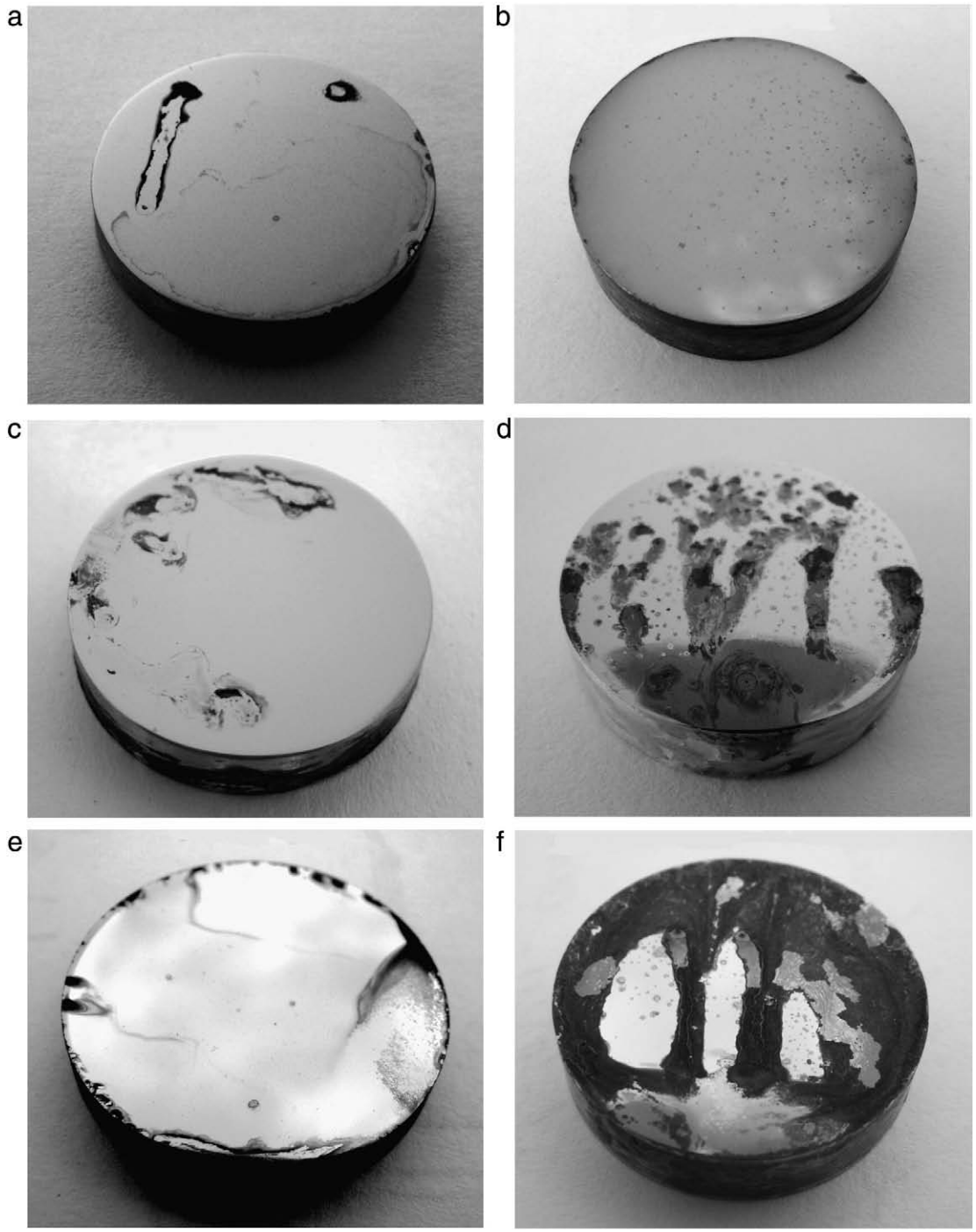

Fig. 4. Photographs of the samples tested in salt spray for 100 h. a) Non nitrided Corrax and b) nitrided; c) non nitrided N695 and d) nitrided; e) non nitrided M340 and f) nitrided.

Table 3
Quantitative analysis of corrosion damage after 100 h salt spray fog test and corrosion potential in open circuit configuration (steady state value).

Sample	Affected area	Number of Pits	E_{corr} [V vs. SCE]
Non Nitr. M340	7%	–	−0.267
Nitrided M340	62%	6	−0.375
Non Nitr. N695	4%	–	−0.370
Nitrided N695	28%	40	−0.495
Non Nitr. Corrax	<1%	–	−0.180
Nitrided Corrax	2%	–	−0.184

and no nitrided samples at lower potentials. At intermediate potentials, nitrided samples showed current fluctuations that could be related to metastable localized corrosion. Again, E_{50} potentials were lower for nitrided samples (Fig. 5b). No localized corrosion was found under the O-ring and neither was possible to find pits on the surface that could explain the observed current fluctuations and the differences between nitrided and non nitrided samples in the anodic curves.

In order to go further in the corrosion behavior understanding of nitrided Corrax steel, cyclic potentiodynamic polarization tests were performed on treated and non treated samples. Results are presented in Fig. 6 and again it can be observed that in the passivity range

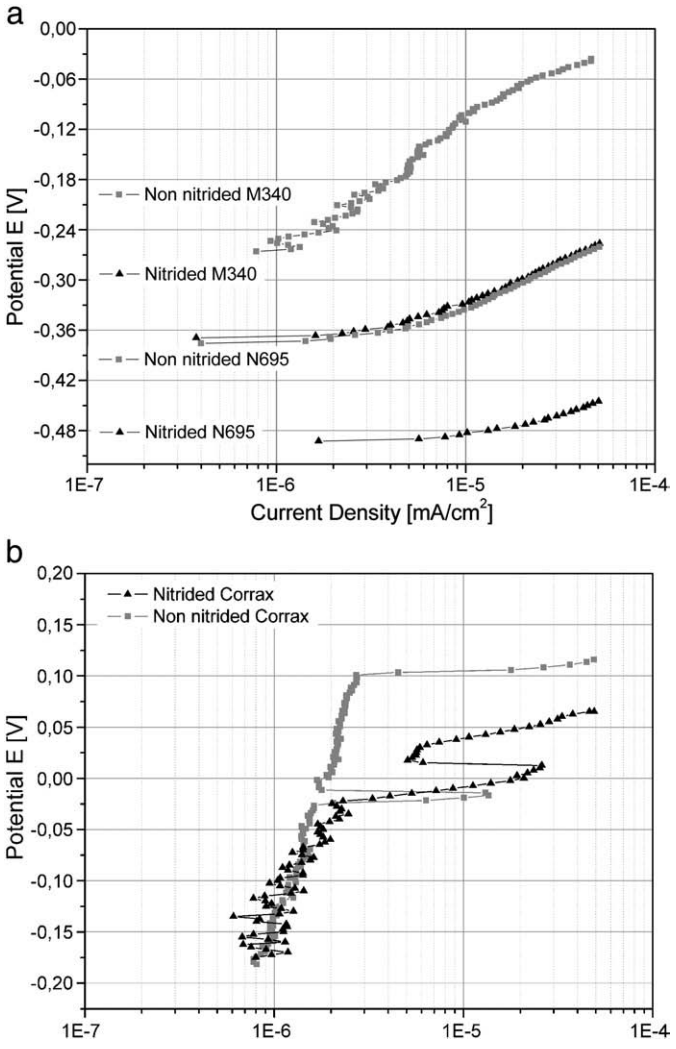

Fig. 5. Anodic polarization curves of all samples. a) M340 and N695, b) Corrax.

nitrided samples have higher currents and a lower E_{200}. Repassivation potential E_r is more negative in the case of nitrided samples than that of non nitrided ones. Moreover, under the tested conditions E_r is negative respect the E_{corr} indicating that the surface treatment could have a somewhat detrimental effect for localized corrosion resistance.

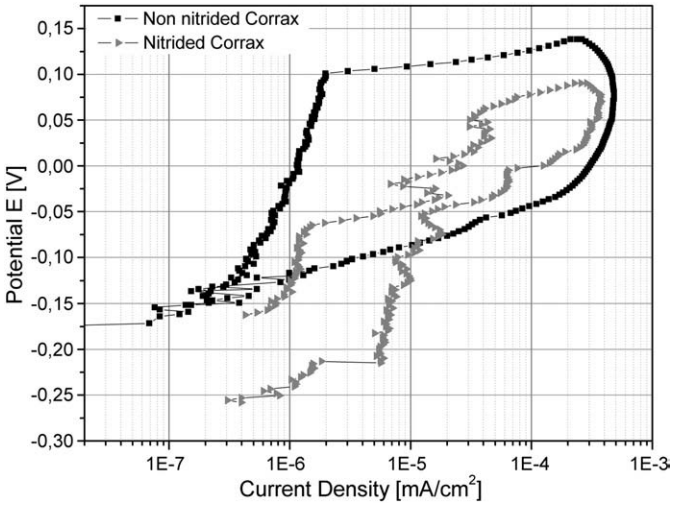

Fig. 6. Cyclic potentiodynamic polarization of Corrax samples.

4. Discussion

The results of the glancing angle XRD analysis were consistent with several papers that reported that the white layer in nitrided martensitic steels is a stressed structure called "expanded martensite" [19–21], where nitrogen is present on interstitial sites of the bcc ferrite tetragonally distorted lattice (as it has been indicated above, "expanded ferrite" could be a more appropriate name for this structure). This layer provides high hardness, even if it is only 10–12 μm thick as it is the case of nitrided Corrax. The formation of dark sublayers on the surface is associated with the chromium nitrides formation, a chromium depletion in solid solution and as a consequence, a bad corrosion resistance in martensitic stainless steels [7,8]. Since no dark sublayers or regions were observed in the micrographs, the treatment was thought to be suitable for corrosion purposes in all the studied steels. However, the first corrosion test, the $CuSO_4 \cdot 5H_2O$ spot, indicated that passivation was not optimum in the case of nitrided M340 and N695. Only nitrided Corrax showed no copper deposition and also an acceptable corrosion resistance in the salt fog spray test. Finally, electrochemical tests were carried out and it was found that nitriding had a detrimental effect in all these steels. It was showed that martensitic stainless steels M340 and N695 had a bad passive behavior, because high anodic currents were observed along the tested potential range in both non nitrided and nitrided steels. Corrax samples, on the contrary, underwent a typical transition course from self-passivation to localized corrosion in this chloride solution. Nitrided Corrax samples had also a passive behavior with metastable localized corrosion at higher potentials. E_{200} potential values were much lower indicating a decrease in the protective film quality formed on nitrided samples.

The corrosion resistance reduction in the martensitic steels N695 and M340 could be related to chromium depletion, initiated during the heat treatment with the formation of Cr carbides. Corrosion resistance gets worse if Cr nitrides are formed during the nitriding process and in fact, those carbides and nitrides were observed in XRD analysis of M340 and especially in N695 nitrided samples. When the matrix contains a fine dispersion of low chromium carbides, corrosion resistance normally remains invariable [21–24] but when chromium-rich carbides of type $Cr_{23}C_6$ are formed, corrosion resistance is diminished. These carbides could be observed as white islands, below the nitrided layer, in the micrographs of nitrided samples from N695 and M340 steels (Fig. 1b and c), indicating that they were formed in the heat treatment stage.

In the nitriding process, it was reported that CrN formation occurs near the precipitated Cr carbides, in the vicinity of grain boundaries, enhancing the probability of localized corrosion to occur [8], as it was observed in this study. Confirmation was assessed by the EDS analysis of these precipitates indicating that they are mostly located in grain boundaries and presented a high Cr concentration. It is probable then that chromium was depleted due to carbide and nitride formation and therefore the Cr content in the surrounding matrix was lower than the minimum needed to ensure an acceptable corrosion resistance all over the surface (11–12%).

In the case of Corrax, the corrosion resistance reduction was not so remarkable, mainly because it is a low carbon steel and only very fine and few chromium precipitates were formed during the aging treatment [18].

5. Conclusion

Corrosion resistance of martensitic stainless steels M340 and N695 could not be sustained after nitriding treatment, even carried out at low temperature, 360 °C. Corrax samples showed a better behavior, but nitride samples showed not as good corrosion performance as the non treated ones.

In the case of martensitic stainless steels, more research has to be done to avoid chromium depletion even before plasma nitriding, in the heat treatment condition. In the case of the precipitation hardening steel Corrax, a good corrosion behavior could be achieved with a better control of other nitriding process parameters than temperature, for example diminishing the nitrogen content in the gaseous mixture for nitriding or the nitrogen activity by current density control.

Acknowledgements

This work was financially supported by the National University of Technology (PID 25D/031), the firm IONAR S.A (Buenos Aires) and the National University of Mar del Plata.

The authors want to thank Uddeholm and Boehler for the materials provided for this study, also the collaboration of Eduardo González from Concepción del Uruguay, for the salt spray fog apparatus and tests; Eugenia Dalibón from UTN-FRCU for her collaboration in hardness measurements and XRD analysis, Lisandro Escalada from UNMdP for his collaboration in the corrosion experiments and Belen Parodi from the Microscopy Lab. of National Institute of Technology for the Industry (INTI), Argentina.

References

[1] T. Bell, Y. Sun, Surf. Eng. 6 (1990) 133.
[2] M.P. Fewell, D.R.G. Mitchell, J.M. Priest, K.T. Short, G.A. Collins, Surf. Coat. Technol. 131 (2000) 300.
[3] T. Czerwiec, H. He, S. Weber, C. Dong, H. Michel, Surf. Coat. Technol. 200 (2006) 5289.
[4] E. De Las Heras, P. Corengia, M. Brizuela, A. García-Luis, G. Ybarra, N. Mingolo, A. Cabo, S.P. Brühl, Plasma Process. Polym. 4 (2007) 5741.
[5] A. Fossati, F. Borgioli, E. Galvanetto, T. Bacci, Corros. Sci. 48 (2006) 1513.
[6] X. Li, T. Bell, Corros. Sci. 46 (2004) 1527.
[7] A. Fossati, F. Borgioli, E. Galvanetto, T. Bacci, Corr. Sci. 48 (2006) 1513.
[8] C.X. Li, T. Bell, Corros. Sci. 48 (2006) 2036.
[9] C.E. Pinedo, W.A. Monteiro, Surf. Coat. Technol. 179 (2004) 119.
[10] Y.-T. Xi, D.-X. Liu, D. Han, Surf. Coat. Technol. 202 (2008) 2577.
[11] M. Esfandiari, H. Dong, Surf. Coat. Technol. 202 (2007) 466.
[12] F. Calosso, C. Ernst, U. Huchel, in Proc. 7th Int. Tooling Conference: Tooling materials and their applications from research to market, Turin, Italy 2–5 May 2006.
[13] S.P. Brühl, R. Charadia, C. Sanchez, M.H. Staia, Int. J. Mater. Res. 7 (2008) 779.
[14] ASM Handbook, Metallography and Microstructures, vol. 9, ASM International, 1998.
[15] ASTM B117, Standard Practice for Operating Salt Spray (Fog) Apparatus, ASTM International, 2007.
[16] S. Simison, S.R. de Sánchez, D.J. Schiffrin, Corrosion 45 (1989) 12.
[17] ASM Handbook, Corrosion, vol. 13, ASM International, 1998.
[18] P. Kochmanski, J. Nowacki, Surf. Coat. Technol. 202 (2008) 4834.
[19] R. Frandsen, Th. Christiansen, M.A.J. Somers, Surf. Coat. Technol. 200 (2006) 5160.
[20] D. Manova, G. Thorwarth, S. Mändl, H. Neumann, B. Stritzker, B. Rauschenbach, Nucl. Instrum. Meth. B 242 (2006) 285.
[21] J.-Y. Park, Y.-S. Park, Mater. Sci. Eng. A 449–451 (2007) 1131.
[22] G. Li, J. Wang, C. Li, Q. Peng, J. Gao, B. Shen, Nucl. Instrum. Meth. Phys. Res. B 266 (2008) 1964.
[23] T.P. Savas, A.Y.L. Wang, J.C. Earthman, J. Mater. Eng. Perform. 12 (2003) 165.
[24] D.W. Hetzner, W. Van Geertruyden, Mater. Char. 59 (2008) 825.